

# Determination of Spin and CP-Eigenvalue of the Higgs Boson with ATLAS

C. P. Buszello<sup>\*</sup> I. Fleck<sup>†</sup> P. Marquard<sup>‡</sup> J. J. van der Bij<sup>§</sup>

*Albert-Ludwigs-Universität*

*Fakultät für Mathematik und Physik, Physikalisches Institut,  
Hermann-Herder-Straße 3, D-79104 Freiburg Germany*

December 24, 2018

## Abstract

A possibility to prove spin and CP-eigenvalue of a Standard Model (SM) Higgs boson is presented. We exploit angular correlations in the subsequent decay  $H \rightarrow ZZ \rightarrow 4l$  (muons or electrons). We compare the angular distributions of the leptons originating from the SM Higgs with those resulting from decays of hypothetical particles with differing quantum numbers. This decay channel is the most promising one for Higgs searches at the LHC. We restrict our analysis to the use of the Atlas-detector which is one of two multi-purpose detectors at the upcoming 14 TeV proton-proton-collider (LHC) at CERN. By applying a fast simulation of the Atlas detector it can be shown that these correlations will be measured sufficiently well to prove consistency with the parameters of the Standard Model Higgs. Although the method is valid for all Higgs masses, we focus on the mass range above 200 GeV, where the branching ratio to ZZ is high enough to perform the measurement at an integrated luminosity of  $100 \text{ fb}^{-1}$ .

---

<sup>\*</sup>buszello@cern.ch

<sup>†</sup>Ivor.Fleck@cern.ch

<sup>‡</sup>marquard@physik.uni-freiburg.de

<sup>§</sup>jochum@phyv1.physik.uni-freiburg.de

# 1 Introduction

Although the standard  $SU(2)_L \times U(1)_Y$  electroweak gauge theory successfully explains all current data, the mechanism of spontaneous symmetry breaking has been tested only partially. Since in the Standard Model spontaneous symmetry breaking is due to the Higgs sector, the search for a Higgs particle will be one of the main tasks of future colliders.

At present, LEP gives a lower limit of about 114 GeV [1] for the Higgs boson mass. For larger values of  $m_H$  one has to consider high energy hadron colliders such as the LHC ( pp collisions at  $\sqrt{s} = 14$  TeV ). A Standard Model Higgs boson lying below the  $WW$  threshold will mainly decay into a  $b\bar{b}$  pair. In this case there is an overwhelming direct QCD background which dominates the signal. In this mass region the Higgs boson is therefore difficult to study in detail, even though one can use rare decays as a signal. Rare decays considered in the literature include, for example,  $H \rightarrow \tau^+ \tau^-$ ,  $H \rightarrow \gamma\gamma$ ,  $H \rightarrow Z\gamma$ ,  $H \rightarrow ZZ^*$  or  $H \rightarrow WW^*$ . All of these signals are rather difficult to see, but can eventually be used to establish the existence of the Higgs boson [2]. While these decay modes can be used to discover the Higgs boson, a detailed study of its properties will be difficult due to statistics and can only be attempted when the full luminosity at the LHC is available.

The situation is much better for heavy Higgs bosons ( $m_H > 2m_W$ ). For such a Higgs boson the main decay products are vector boson pairs,  $W^+W^-$  or  $ZZ$ . A clear signal for the Higgs then consists of a peak in the invariant mass spectrum of the produced vector bosons. The double leptonic decay of the  $Z$  boson,  $H \rightarrow ZZ \rightarrow l^+l^-l^+l^-$ , leads to a particularly clean signal.

In this case the basic strategy for discovering a Higgs boson in a clean mode, is to trigger on 4 high  $p_T$  leptons that can be combined to form two  $Z$ -bosons. Here,  $30 \text{ fb}^{-1}$  is already sufficient. If one finds such a signal one might be tempted to assume this to be the Standard Model Higgs boson. However given the fact that the Higgs sector is not fully prescribed, one has to allow for other possibilities. In strongly interacting models, for instance, low lying (pseudo)-vector resonances are possible[3, 4]. Also pseudoscalar particles are present in a variety of models [5]. Therefore, the first priority after finding a signal is to establish the nature of the resonance, in particular its spin and CP-eigenvalue. This can be done by studying angular distributions and correlations among the decay leptons. In the following, we will make this study. We will limit ourselves to (pseudo)-vector and (pseudo)-scalar particles. We will compare the angular distributions, assuming the production rate of a Standard Model Higgs boson for the different particles. This is, of course not realistic, especially for the vector particles, since they cannot be produced by gluon fusion, due to Yang's theorem[12]. However, it is the

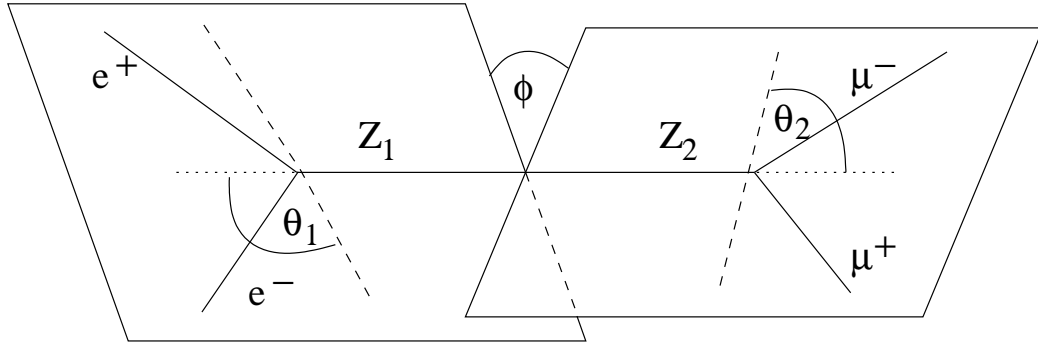


Figure 1: The decay plane angle  $\phi$  is measured between the two planes defined by the leptons from the decay of the two  $Z$  bosons in the rest frame of the Higgs, using the charge of the leptons, to fix the orientation of the planes. The dashed lines represent the direction of motion of the leptons in the rest frame of the  $Z$  Boson from which they originate. The angles  $\theta_1$  and  $\theta_2$  are measured between the negatively charged leptons and the direction of motion of the corresponding  $Z$  in the Higgs boson rest frame.  $\phi=0$  correspond to  $p_{e^+} \times p_{e^-}$  and  $p_{\mu^+} \times p_{\mu^-}$  being parallel.  $\phi=\pi$  correspond to  $p_{e^+} \times p_{e^-}$  and  $p_{\mu^+} \times p_{\mu^-}$  being antiparallel.

correct comparison to make, if one wants to prove that the signal found is indeed the Standard Model Higgs particle, with the correct quantum numbers.

Theoretical studies of angular distributions have been performed in the literature [6-11]. So far, such studies have been limited to theoretical discussions. However it was shown in [10], that acceptance and efficiencies of the detector can play a role, since they can generate correlations, mimicking physical ones. Therefore, it is necessary to use a detector simulation in order to establish how well one can do in practice.

The complete triple differential cross sections can be calculated and are given in the appendix, but they are not very enlightening and we will limit ourselves to the most important integrated angular distributions. For the definition of the angles see Figure 1.

There are essentially two distributions that we study. One is the distribution of the cosine of the polar angle,  $\cos \theta$ , of the decay leptons relative to the  $Z$  boson. Because the heavy Higgs decays mainly into longitudinally polarised vector bosons the cross section  $d\sigma/d\cos \theta$  should show a peaking near zero. The other is the distribution of the angle  $\phi$  between the decay planes of the two  $Z$  bosons in the rest frame of the Higgs boson. This distribution depends on the details of the Higgs decay mechanism. Within the Standard Model a behaviour

roughly like  $1 + \beta \cos 2\phi$  is expected. This last distribution is flattened in the decay chain  $H \rightarrow ZZ \rightarrow 4l$ , because of the small axial vector coupling of the leptons, in contrast to the decay into W's or quarks. Also, cuts can significantly affect the correlations. Therefore one needs a precise measurement of the momenta of the outgoing leptons. The Atlas-detector is very well suited to measure these distributions, since the muon and electron reconstruction is very precise. A detector Monte-Carlo is however needed in order to determine whether the angular distributions can be measured sufficiently well in order to determine the quantum numbers of the Higgs particle.

The present paper is organized as follows. In Chapter 2 the generator is described, in Chapter 3 detector simulation and reconstruction are given. In Chapter 4 we define quantities that can be used to characterize the different distributions. In Chapter 5 we present the results, concluding that the quantum numbers of the Higgs particle can indeed be determined. In the appendix we give formulas for the complete differential and integrated distributions for the decay of the resonance assuming arbitrary couplings.

## 2 The Generators

In order to distinguish between different spins  $J=0,1$  and/or CP-eigenvalues  $\gamma_{CP} = -1, +1$  one needs to study four different distributions, which result from the decay of the Standard Model Higgs boson plus three different alternative, hypothetical particles that behave like the Higgs boson, but which decay as if they were particles with  $J = 0$  and  $\gamma_{CP} = -1$ ,  $J = 1$  and  $\gamma_{CP} = +1$ , or  $J = 1$  and  $\gamma_{CP} = -1$ .

The feasibility of using angular correlations in the decay of the Z bosons in order to distinguish between these particles has been evaluated using two different Monte-Carlo generators. One was written by T. Matsuura and J.J. van der Bij [10] for the Standard Model Higgs ( $gg \rightarrow H \rightarrow ZZ \rightarrow 4l$ ) and the irreducible ZZ-background. The latter includes contributions from both gluons and quarks to the ZZ production ( $gg \rightarrow ZZ \rightarrow 4l$  and  $q\bar{q} \rightarrow ZZ \rightarrow 4l$ ), whereas all Higgs production mechanisms other than the gluon fusion are neglected. This generator, unlike other popular programmes, keeps all polarisations of the Z-boson, including the gluon initiated process. This allows for an analysis of the angular distributions of the leptons. The gluonic production of Z-boson pairs is only about 30% of the total background. Therefore at the Higgs peak its effect tends to be small. However one should not ignore its contribution, since it has different angular distributions from the other background and its presence can effect measured correlations. The programme contains no K-factors, therefore our conclusions regarding the feasibility of the determination of Higgs quantum numbers are conservative. Since the narrow width approximation is used, the

results are only valid for Higgs masses above the ZZ threshold.

For the alternative particles, a new generator was written based on an article by C. A. Nelson and J. R. Dell' Aquilla [9]. Both generators use Cteq4M structure functions [13] and hdecay [14] for branching-ratio and width of the Higgs, and both use the narrow width approximation. Doing the analysis after the start of the LHC requires the detection of a particle with a mass above 180 GeV and the appropriate width and branching ratios to fulfill the minimum requirement for being recognized as a Standard Model like Higgs. Since the production mechanism (gluon-fusion rules out spin 1 particles) cannot be seen, the only way to prove that the spin and CP nature of the new particle is Standard Model like is to study the decay angles of the leptons. In order to anticipate this required measurement, we assume that all four particles are produced in a way that gives rise to the same mass and width. The background as well as all cross sections for the four simulations are taken from the first generator. Thus, all cases show identical distributions of invariant mass of the Z-pairs and transverse momentum  $P_T$  of Z-bosons and leptons and have the same width and cross sections. The only difference lies in the angular distributions of the leptons. For the alternative particles no special assumption concerning the coupling has to be made; only CP-invariance is assumed. It is worth mentioning that the angular correlations are completely independent of the production mechanism.

### 3 Detector Simulation and Reconstruction

The detector response is simulated using ATLFast [15], a software-package for particle level simulation of the Atlas detector. It is used for fast event-simulation including the most crucial detector aspects. Starting from a list of particles in the event, it provides a list of reconstructed jets, isolated leptons and photons and expected missing transverse energy. It applies smearing and efficiencies to all reconstructed particles, with the amount and distribution of these parameters mostly taken from a full simulation using Geant3 [16].

The event selection is modeled exactly after the event selection in the Atlas-Physics-TDR [17]. Four leptons (electrons or muons) are required in the pseudo-rapidity range  $|\eta| = |-\ln \tan(\frac{\theta}{2})| < 2.5$  ( $\theta$  being the angle to the beamline). Two of the leptons are required to have transverse momenta greater than 20 GeV and the two other leptons must have transverse momenta greater than 7 GeV each. Two Z bosons are reconstructed by choosing lepton-pairs of matching flavour and opposite sign. If the flavours of all four leptons are equal, the combination is chosen, which simultaneously minimizes the deviation of the invariant mass of the pairs with opposite sign from the Z mass. The reconstructed invariant mass

### Polar angle distributions of signal and background

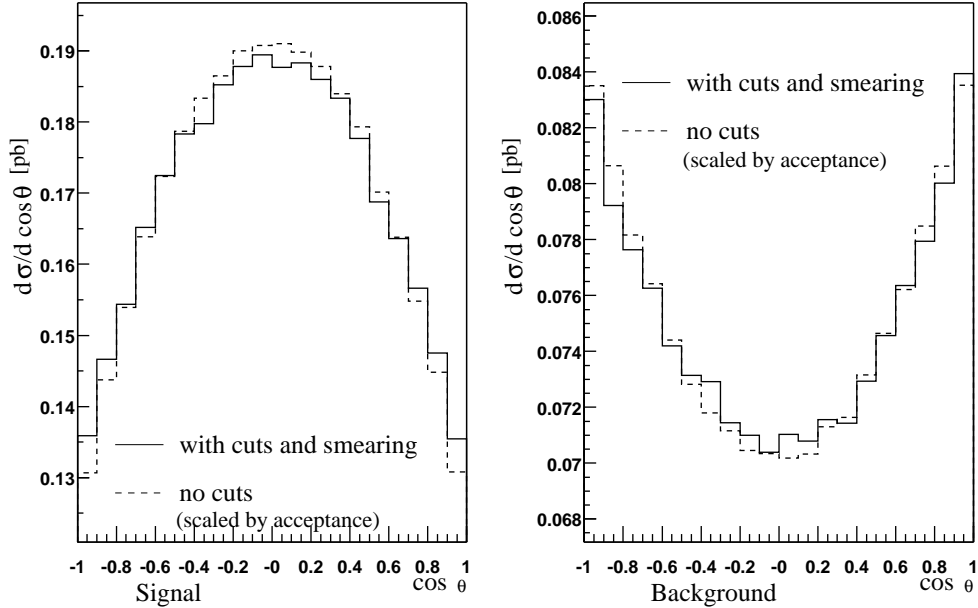


Figure 2: Distribution of the polar angle  $\cos(\theta)$  for the background only (right) and the signal (left). The Higgs mass is 200 GeV.

of the two reconstructed Z bosons has to lie within two times the width of the reconstructed mass peak of the Higgs resonance around the center of the peak. For high Higgs masses ( $m_H > 300$  GeV) this is only little more than two times the decaywidth, while for smaller masses the experimental resolution dominates.

Throughout this paper, we use the term signal for distributions where the background has been statistically subtracted. The only background considered is the Z pair production. Other possible backgrounds like top pair production or Zbb are negligible for masses of the Higgs boson above 200 GeV. Systematic uncertainties due to the simulation of the background could be studied by comparing distributions from the sidebins of the Higgs signal with the results of the generator. A proper treatment of the background is very important, since the angular distributions of the background itself and correlations introduced by detector effects have a large impact on the shape of the distributions discussed. These effects are detailed below.

For high invariant masses, the Z bosons from the background processes are mainly transversely polarised leading to a polar angle distribution of the form

$\frac{d\sigma}{d\cos\theta} \sim 1 + \cos^2\theta$ . This distribution flattens the  $\sin^2\theta$  distribution expected for the Higgs decay. Figure 2 shows the polar angle distributions of the signal (left) and the background (right). The dashed line shows the shape of the distribution expected when no cuts are applied and the detector response is not taken into account. It has just been scaled by the overall acceptance of the cuts, so that the shape can be compared. The expected distribution with all cuts and smearing applied is drawn as a solid line. The Figures 2 and 3 are produced assuming a Higgs mass of 200 GeV and Z decaying to muons only. For the decay into electrons and/or muons the graphs look similar. The smearing effects are largely independent of the mass of the Higgs.

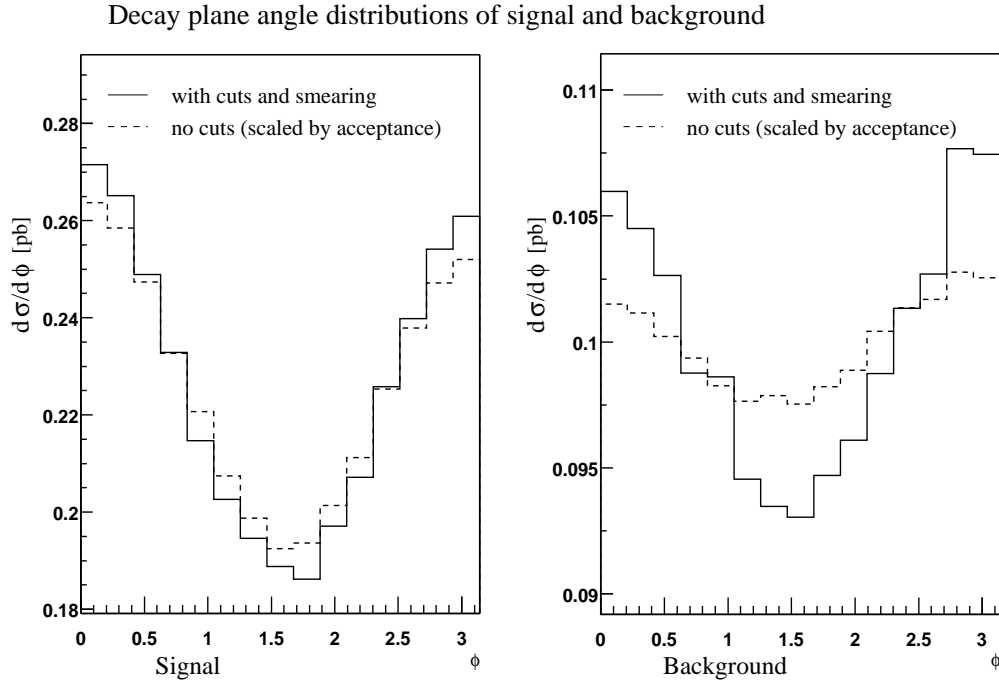


Figure 3: Distribution of the decay plane angle  $\phi$  for the background only (right) and the signal (left). The Higgs mass is 200 GeV. The distribution without cuts is scaled by the expected acceptance, so that the shape can be directly compared.

The effect of the detector for the decay plane angle is shown in Figure 3. Again, the distribution of the signal is shown left and the background on the right. The dashed histograms are scaled to have the same integral as the solid histograms, and zero is suppressed in order to facilitate the comparison of the shape. The definition of the line styles are the same as above. For the decay plane angle, the background shows an almost flat distribution before applying selection cuts. But a minor correlation is introduced by detector effects. This

Spin	$\gamma_{CP}$	
0	-1	$1 - \mathcal{R}P_2(\cos \theta_1) - \mathcal{U}P_2(\cos \theta_2) + \mathcal{R}\mathcal{U}P_2(\cos \theta_1)P_2(\cos \theta_2) + \frac{9}{4}\mathcal{T}\mathcal{W}P_1(\cos \theta_1)P_1(\cos \theta_2)$
1	+1	$1 + \frac{1}{2}\mathcal{R}P_2(\cos \theta_1) + \frac{1}{2}\mathcal{U}P_2(\cos \theta_2) - 2\mathcal{R}\mathcal{U}P_2(\cos \theta_1)P_2(\cos \theta_2)$
1	-1	$1 + \frac{1}{2}\mathcal{R}P_2(\cos \theta_1) + \frac{1}{2}\mathcal{U}P_2(\cos \theta_2) - 2\mathcal{R}\mathcal{U}P_2(\cos \theta_1)P_2(\cos \theta_2)$

Table 1: Distribution of the polar angle  $\theta$ .  $P_i$  are the Legendre Polynomials. See the text for definitions.

has been simulated and taken into account for the analysis of decay plane angle distributions. The cuts isolating the signal lead to a distortion of the angular distributions as discussed in [10], but they are almost negligible for the Atlas detector. The cut on  $|\eta|$  enhances the decay plane correlation a little, but the smearing and the  $P_T$  requirements reduce this effect. Altogether, there is a small enhancement of the correlation of almost the same amount for all four particles.

A further cut on the transverse momentum of the Z bosons  $P_T^{max}(Z_1, Z_2) > m_H / 3$  is known to additionally reduce the background, but it also affects the correlation. Since an optimisation of the signal-to-background ratio is not crucial to this analysis, this cut has not been applied, offering the advantage of being less dependent on the details of the production mechanism like initial  $P_T$  of the Higgs boson.

## 4 Parametrisation of Decay Angle Distributions

The differential cross sections for the different models can be computed directly or can be derived from the formulas given in [9]. The explicit distributions are given in the appendix. From the article [9] we quote the simple distributions of the alternative particles. Table 1 shows the distribution of the polar angle  $\theta$ .  $\theta_1$  and  $\theta_2$  are the polar angles of the leptons originating from the Z Bosons  $Z_1$  and  $Z_2$ , respectively. In Table 2 the distribution of the decay plane angle  $\phi$  is shown where the polar angle  $\theta$  is integrated over different ranges. F11 gives the distribution for  $0 \leq \theta_{1,2} \leq \pi/2$ , F22 for  $\pi/2 \leq \theta_{1,2} \leq \pi$ , F12 for  $0 \leq \theta_1 \leq \pi/2$  and  $\pi/2 \leq \theta_2 \leq \pi$ , and F21 for  $\pi/2 \leq \theta_1 \leq \pi$  and  $0 \leq \theta_2 \leq \pi/2$ .  $\mathcal{R}$ ,  $\mathcal{U}$ ,  $\mathcal{T}$  and  $\mathcal{W}$  are the parameters that characterise the decay density matrix. For the decay modes used in this analysis they amount to the following values:  $\mathcal{R} = \mathcal{U} = -1/2$ ,  $\mathcal{T} = \mathcal{W} = -\frac{2r}{1+r^2}$ .  $r$  is the ratio of the axial vector to vector coupling which for the muons amounts to  $r = (1 - 4 \sin^2 \theta_W)^{-1}$ . We used  $\sin^2 \theta_W = 0.23$ .

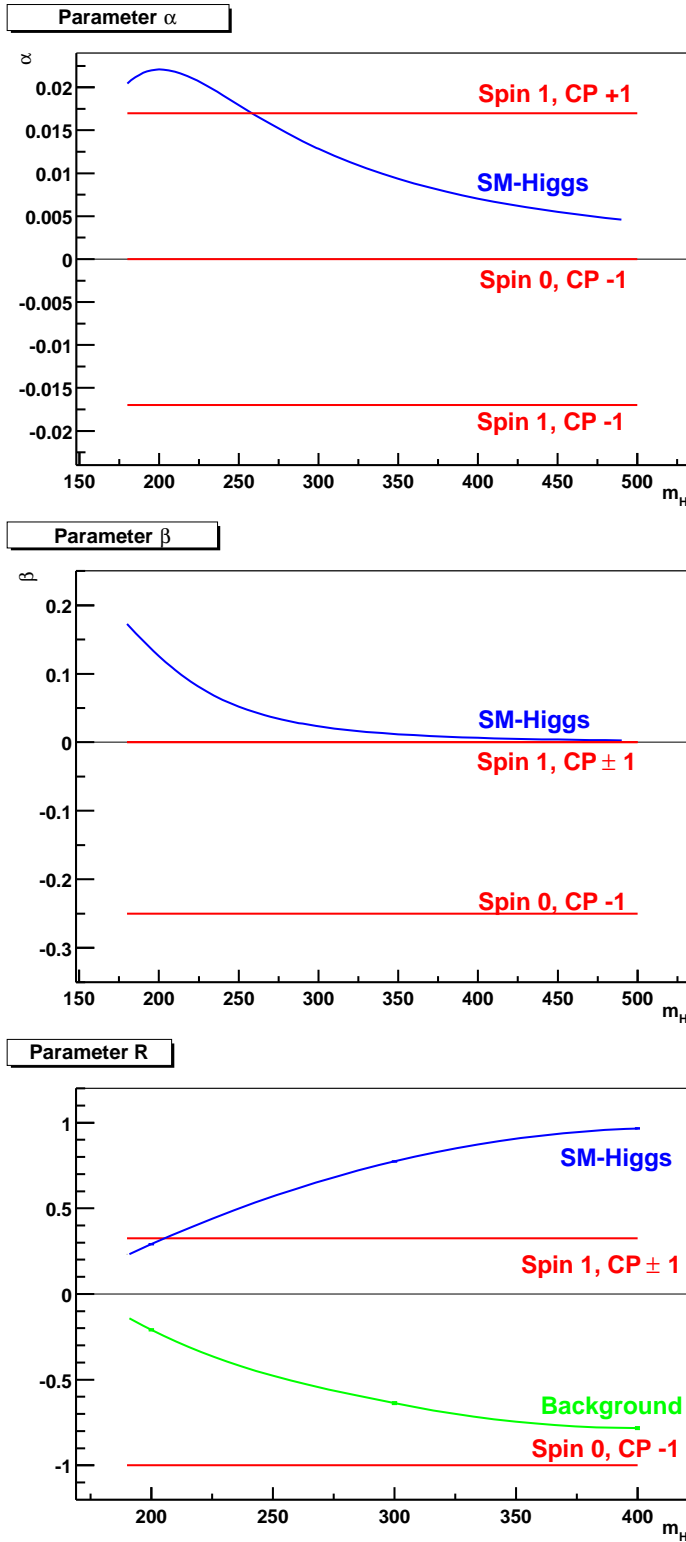


Figure 4: The variation of the three parameters  $\alpha$ ,  $\beta$  and  $R$  (top to bottom) with the Higgs mass.

Spin=0 $\gamma_{CP}=-1$	
F11 + F22	$1 + \frac{9}{16}\mathcal{T}\mathcal{W} - \mathcal{R}\mathcal{U}\cos(2\phi)$
F12 + F21	$1 - \frac{9}{16}\mathcal{T}\mathcal{W} - \mathcal{R}\mathcal{U}\cos(2\phi)$
Spin=1 $\gamma_{CP}=+1$	
F11 + F22	$1 + (-\frac{1}{2}\mathcal{R}\mathcal{U} + \frac{1}{2}\mathcal{T}\mathcal{W}(\frac{3\pi}{8})^2)\cos(\phi)$
F12 + F21	$1 + (+\frac{1}{2}\mathcal{R}\mathcal{U} + \frac{1}{2}\mathcal{T}\mathcal{W}(\frac{3\pi}{8})^2)\cos(\phi)$
Spin=1 $\gamma_{CP}=-1$	
F11 + F22	$1 + (+\frac{1}{2}\mathcal{R}\mathcal{U} - \frac{1}{2}\mathcal{T}\mathcal{W}(\frac{3\pi}{8})^2)\cos(\phi)$
F12 + F21	$1 + (-\frac{1}{2}\mathcal{R}\mathcal{U} - \frac{1}{2}\mathcal{T}\mathcal{W}(\frac{3\pi}{8})^2)\cos(\phi)$

Table 2: Distribution of the decay plane angle  $\phi$ . F11 gives the distribution for  $0 \leq \theta_{1,2} \leq \pi/2$ , F22 for  $\pi/2 \leq \theta_{1,2} \leq \pi$ , F12 for  $0 \leq \theta_1 \leq \pi/2$  and  $\pi/2 \leq \theta_2 \leq \pi$  F21 for  $\pi/2 \leq \theta_1 \leq \pi$  and  $0 \leq \theta_2 \leq \pi/2$ .  $\mathcal{R} = \mathcal{U} = -1/2$ ,  $\mathcal{T} = \mathcal{W} = -\frac{2r}{1+r^2}$ ,  $r = (1 - 4\sin^2 \theta_W)^{-1}$ .

The plane-correlation can be parametrised as

$$F(\phi) = 1 + \alpha \cdot \cos(\phi) + \beta \cdot \cos(2\phi) \quad (1)$$

In all four cases discussed here, there is no  $\sin(\phi)$  or  $\sin(2\phi)$  contribution. For the Standard Model Higgs,  $\alpha$  and  $\beta$  depend on the Higgs mass while they are constant over the whole mass range in the other cases.

The polar angle distribution can be described by

$$G(\theta) = T \cdot (1 + \cos^2(\theta)) + L \cdot \sin^2(\theta) \quad (2)$$

reflecting the longitudinal or transversal polarisations of the Z boson. We define the ratio  $R := (L - T)/(L + T)$  of transversal and longitudinal polarisation.

The dependence of the parameters  $\alpha$ ,  $\beta$  and  $R$  on the Higgs mass is shown in Figure 4. The pseudoscalar shows the largest deviation from the SM Higgs. It would have  $\beta = -0.25$  and  $R = -1$  whereas the scalar always has  $\beta > 0$  and  $R > 0$ . The vector and the axialvector can be excluded through the parameter  $R$  for most of the mass range, but for Higgs masses around 200 GeV the main difference lies in the value of  $\alpha$  which is close to zero for the scalar, but about  $\pm 0.038$  for  $J=1$  and  $\gamma_{CP} = \pm 1$ . The values for  $\beta$  differ as well, but both are small.

## 5 Results

In the previous section the exact results for the signal were given. However in practice one needs a procedure to separate signal from background, which will

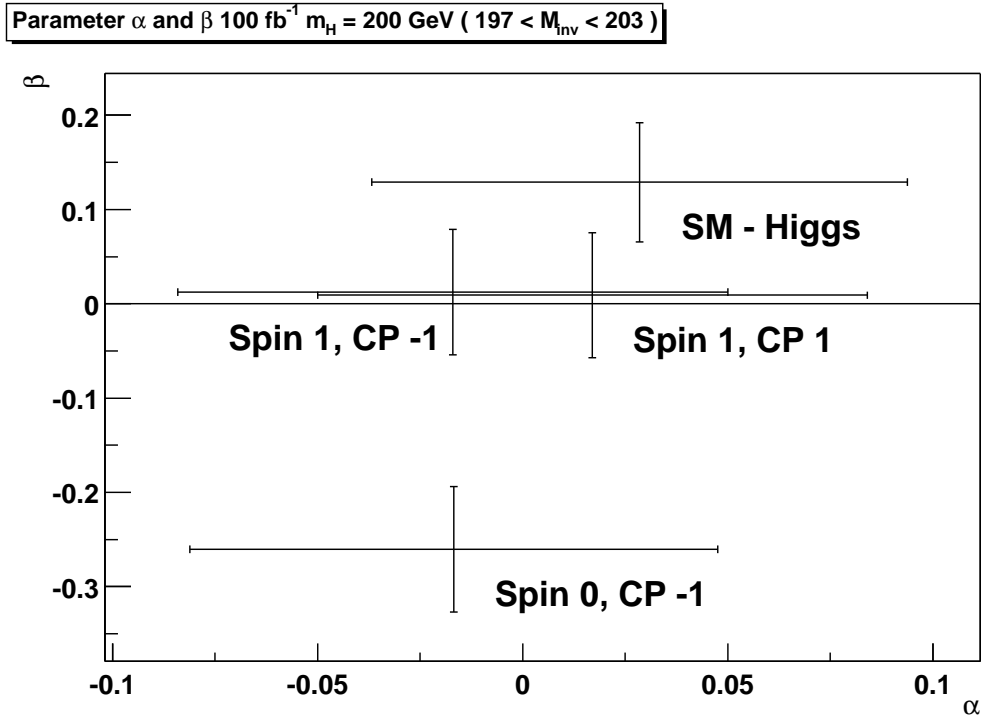
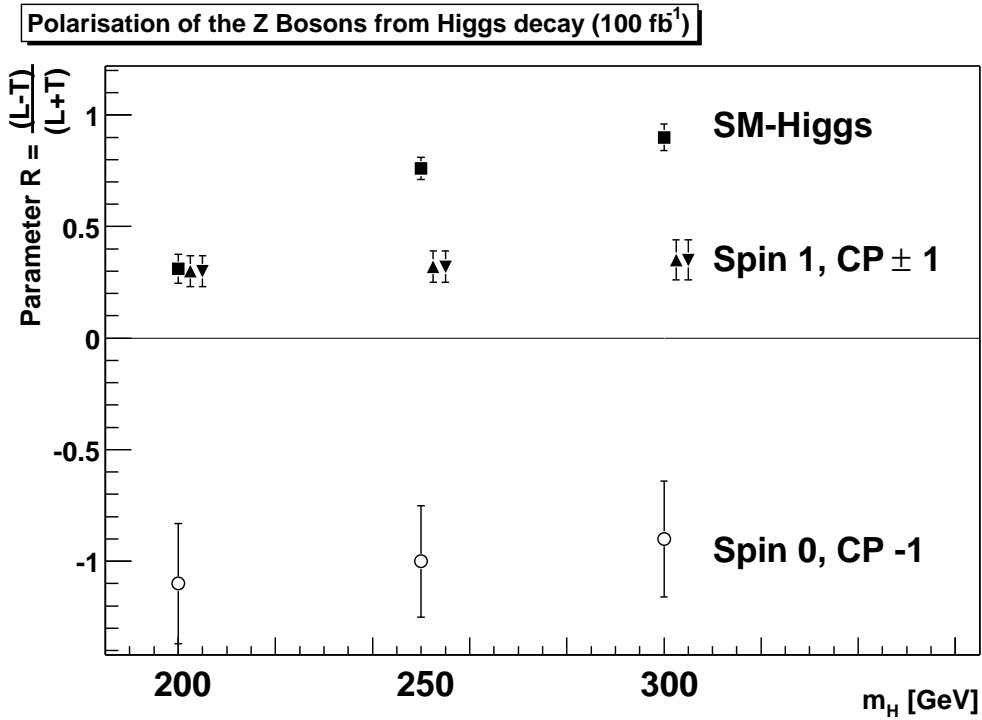
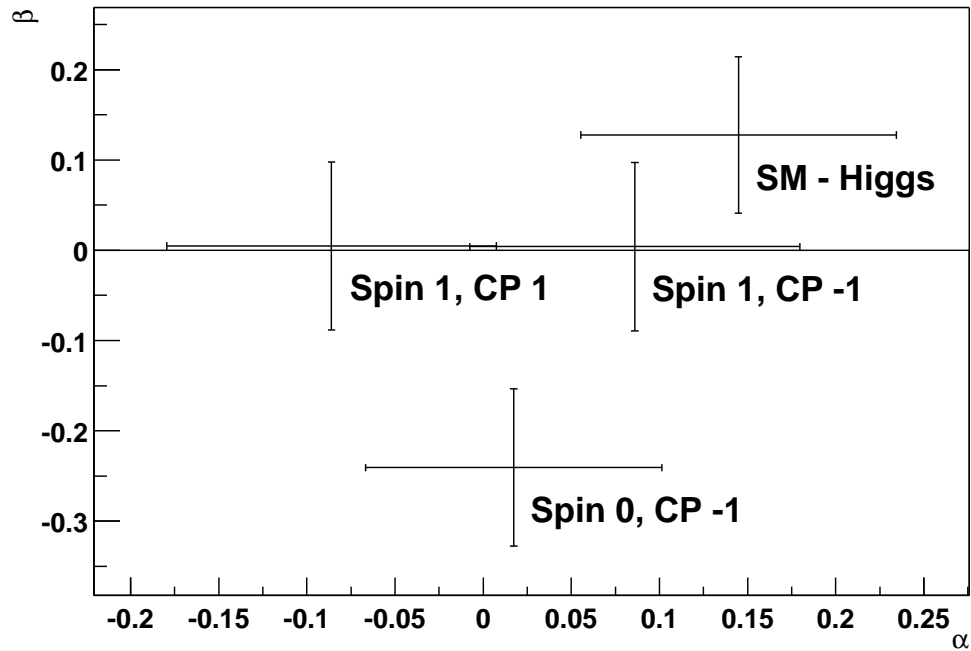


Figure 5: The parameter  $R$  for different Higgs masses (top) and  $\alpha$  and  $\beta$  (bottom) for  $m_H = 200$  GeV using 100  $\text{fb}^{-1}$ . The error scales with the integrated luminosity as expected.

Parameter  $\alpha$  and  $\beta$   $100 \text{ fb}^{-1}$   $m_H = 200 \text{ GeV}$  ( $197 < M_{\text{inv}} < 203$ )



Parameter  $\alpha$  and  $\beta$   $100 \text{ fb}^{-1}$   $m_H = 200 \text{ GeV}$  ( $197 < M_{\text{inv}} < 203$ )

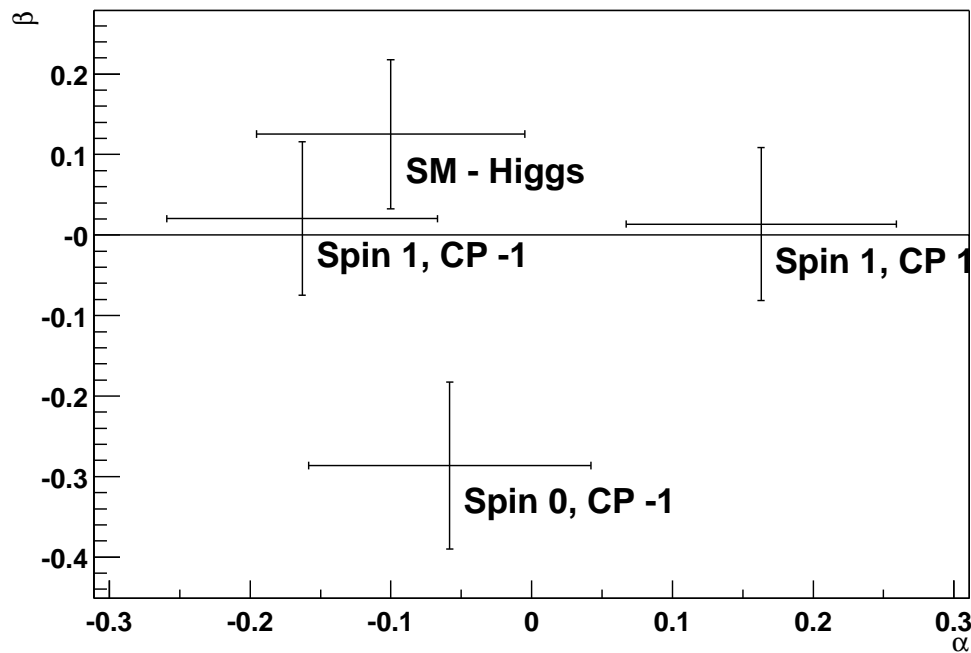


Figure 6: The parameter  $\alpha$  depends on the signs of the  $\cos(\theta)$  of the two Z bosons. The events where the signs are equal are used for the upper plot, those where the signs are different are used for the lower plot.

lead to uncertainties in the distributions. The expected errors have been calculated by generating a large number of events and scaling the distributions to the expected number of events, since the expected values of the parameters follow a Gaussian distribution. The background was statistically subtracted after applying the same cuts to it as were applied to the signal. Then the parametrisations for  $\phi$  and  $\theta$  as described above were fitted to the distributions. Signal and background are summed over muons and electrons.

Figure 5 (top) shows the expected values and errors for the parameter  $R$ , using an integrated luminosity of  $100 \text{ fb}^{-1}$ . It is clearly visible, that for masses above  $250 \text{ GeV}$  this parameter excludes all non Standard Model particles. For a Higgs mass of  $200 \text{ GeV}$  only the pseudoscalar is excluded. Figure 5 (bottom) shows the expected values and errors for  $\alpha$  and  $\beta$  for a  $200 \text{ GeV}$  Higgs and an integrated luminosity of  $100 \text{ fb}^{-1}$ .

The parameter  $\alpha$  can be used to distinguish between a spin 1 and the SM Higgs particle, but its use is statistically limited. The same applies to the parameter  $\beta$ . Measuring  $\beta$ , which is zero for spin 1 and  $> 0$  in the SM case, can contribute only very little to the spin measurement even if  $m_H$  is in the range where  $\beta$ , in the SM case, is close to its maximum value. Nevertheless,  $\beta$  can be useful to rule out a CP odd spin 0 particle.

The values of  $\alpha$  get more widely separated, when the correlation between the sign of  $\cos(\theta)$  for the two Z Bosons and  $\phi$  is exploited. In Figure 6, we plot the parameters separately for  $\text{sign}(\cos \theta_1) = \text{sign}(\cos \theta_2)$  (F11 + F22 in Table 2) and  $\text{sign}(\cos \theta_1) = -\text{sign}(\cos \theta_2)$  (F12 + F21 in Table 2). As can be seen, the difference in  $\alpha$  becomes bigger for  $J = 1$  and  $\gamma_{CP} = +1$ . For higher masses  $\alpha$  and  $\beta$  of the SM Higgs approach 0; thus only  $\alpha$  can be used to measure the spin. But the measurement of  $R$  compensates this.

Figure 7 shows the significance, i. e. the difference of the expected values divided by the expected error of the SM Higgs. We add up the significance for  $\alpha$  and  $\beta$  exploiting the  $\cos(\theta)$  -  $\phi$  correlation and plot the significance from the polar angle measurement separately. For higher Higgs masses the decay plane angle correlation contributes almost nothing, but the polarisation leads to a good measurement of the parameters spin and CP-eigenvalue.

In conclusion, for Higgs masses larger than about  $230 \text{ GeV}$  the quantum numbers of the Higgs signal can be firmly established already with  $100 \text{ fb}^{-1}$ . For  $m_H$  around  $200 \text{ GeV}$  the distinction is less clear, and one will need the full integrated luminosity of the LHC.

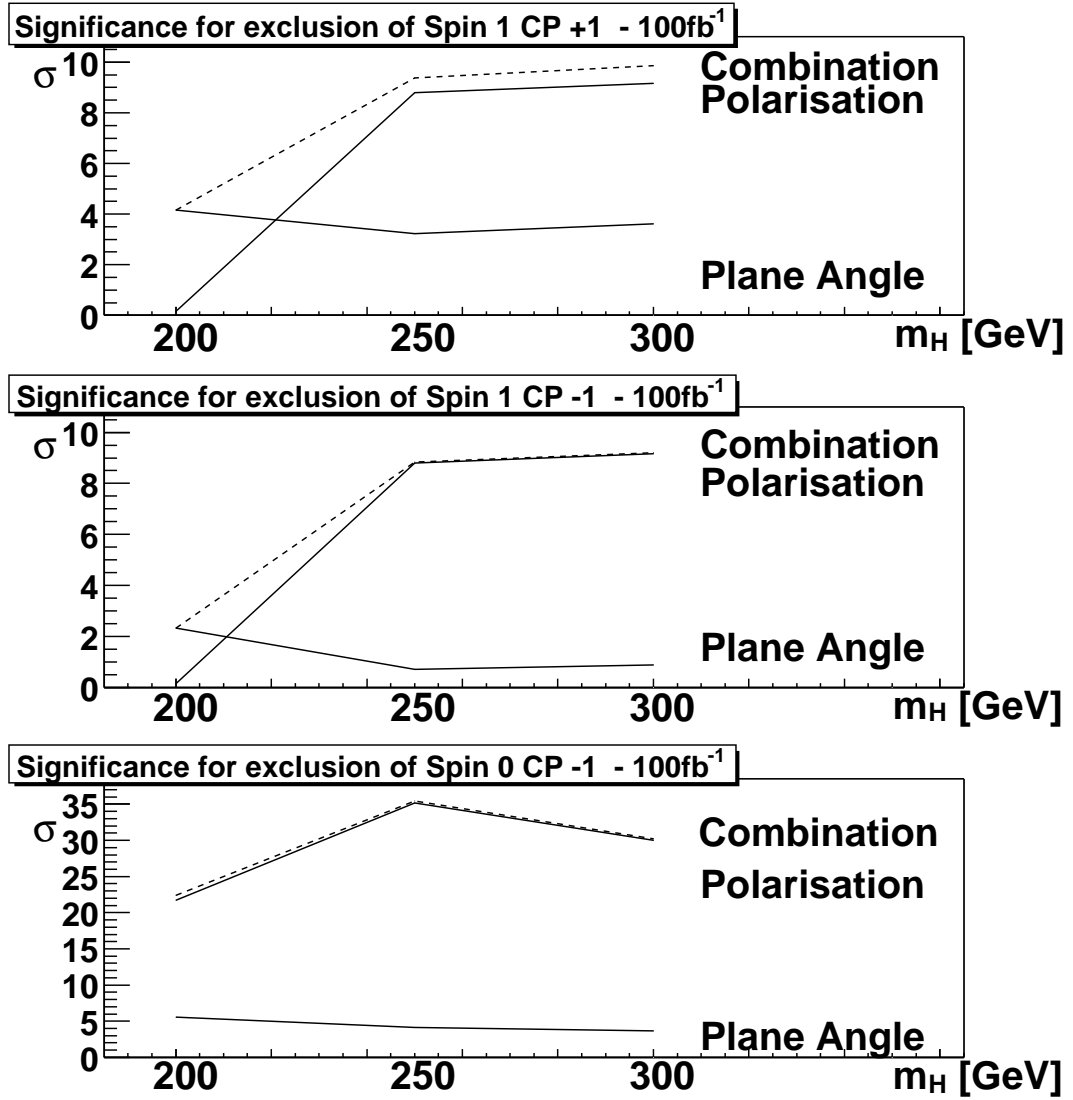


Figure 7: The overall significance for the exclusion of the non standard spin and CP-eigenvalue. The significance from the polar angle measurement and the decay-plane-correlation are plotted separately.

## Acknowledgements

This work was supported by the *DFG-Forschergruppe “Quantenfeldtheorie, Computeralgebra und Monte-Carlo-Simulation”* and by the European Union under contract HPRN-CT-2000-00149.

## A Formulae for differential angular distributions

The most general coupling of a (pseudo) scalar Higgs boson to two on-shell Z-bosons is of the following form:

$$\mathcal{L}_{scalar} = \mathbf{X}\delta_{\mu\nu} + \mathbf{Y}k_\mu k_\nu/M_h^2 + i\mathbf{P}\epsilon_{\mu,\nu,p_Z,q_Z}/M_h^2 \quad (3)$$

Here the momentum of the first Z-boson is  $p_Z^\mu$ , that of the second Z-boson is  $q_Z^\nu$ . The momentum of the Higgs boson is  $k$  and  $\epsilon_{\mu\nu\rho\sigma}$  is the total antisymmetric tensor with  $\epsilon_{1234} = i$ . Within the Standard Model one has  $X = 1$ ,  $Y = P = 0$ . For a pure pseudoscalar particle one has  $P \neq 0$ ,  $X = Y = 0$ . If both  $P$  and one of the other interactions are present, one cannot assign a definite parity to the Higgs boson.

The same formula for a (pseudo) vector with momentum  $k_\rho$  reads:

$$\mathcal{L}_{vector} = \mathbf{X}(\delta_{\rho\mu}p_Z^\nu + \delta_{\rho\nu}q_Z^\mu) + \mathbf{P}(i\epsilon_{\mu,\nu,\rho,p_Z} - i\epsilon_{\mu,\nu,\rho,q_Z}) \quad (4)$$

It is to be noted that the coupling to the vector field actually contains only two parameters and is therefore simpler than to the scalar.

In the following we give the triple differential cross section for the case of a scalar or vector Higgs. The meaning of the angles  $\theta_1, \theta_2$  and  $\phi$  is explained in Figure 1.  $p$  is the absolute value of the momentum of the Z boson,  $p^2 = \frac{1}{2}M_h^2 - M_Z^2$ . In the following we use the definitions  $x = \frac{M_h}{M_Z}$  and  $y = \frac{p}{M_Z}$ .

### A.1 The general case

#### Scalar Higgs

$$\begin{aligned} \frac{d\sigma}{d\phi d\cos\theta_1 d\cos\theta_2} \sim & \\ & - 8\mathbf{XY}c_a^2c_v^2x^2(x^2 - 4)\cos\phi\sin\theta_1\sin\theta_2 \\ & - \mathbf{XY}(c_v^2 + c_a^2)^2x^2(x^2 - 4)(2\cos\phi\sin\theta_1\sin\theta_2\cos\theta_1\cos\theta_2 + (x^2 - 2)\sin^2\theta_1\sin^2\theta_2) \\ & + 16\mathbf{XP}c_a^2c_v^2xy(x^2 - 2)\sin\phi\sin\theta_1\sin\theta_2 \\ & + 4\mathbf{XP}(c_v^2 + c_a^2)^2xy\sin\phi(2\cos\phi\sin^2\theta_1\sin^2\theta_2 + (x^2 - 2)\sin\theta_1\sin\theta_2\cos\theta_1\cos\theta_2) \\ & + 16\mathbf{X}^2c_a^2c_v^2x^2(2\cos\theta_1\cos\theta_2 + (x^2 - 2)\cos\phi\sin\theta_1\sin\theta_2) \\ & + \mathbf{X}^2(c_v^2 + c_a^2)^2x^2\{4(1 + \cos^2\theta_1\cos^2\theta_2 + \cos^2\phi\sin^2\theta_1\sin^2\theta_2 \\ & + (x^2 - 2)\cos\phi\sin\theta_1\sin\theta_2\cos\theta_1\cos\theta_2) + x^2(x^2 - 4)\sin^2\theta_1\sin^2\theta_2\} \\ & - 8\mathbf{PY}c_a^2c_v^2xy(x^2 - 4)\sin\phi\sin\theta_1\sin\theta_2 \\ & - 2\mathbf{PY}(c_v^2 + c_a^2)^2xy(x^2 - 4)\sin\phi\sin\theta_1\sin\theta_2\cos\theta_1\cos\theta_2 \\ & + 1/4\mathbf{Y}^2(c_v^2 + c_a^2)^2x^2(x^2 - 4)^2\sin^2\theta_1\sin^2\theta_2 \\ & + 8\mathbf{P}^2c_a^2c_v^2(x^2 - 4)\cos\theta_1\cos\theta_2 \\ & + \mathbf{P}^2(c_v^2 + c_a^2)^2(x^2 - 4)(1 + \cos^2\theta_1\cos^2\theta_2 - \cos^2\phi\sin^2\theta_1\sin^2\theta_2) \end{aligned}$$

## Vector Higgs

$$\begin{aligned}
& \frac{d\sigma}{d\phi d\cos\theta_1 d\cos\theta_2} \sim \\
& - 16\mathbf{X}\mathbf{P}c_a^2c_v^2xy\sin\phi\sin\theta_1\sin\theta_2 \\
& + 4\mathbf{X}\mathbf{P}(c_v^2 + c_a^2)^2xy\sin\phi\sin\theta_1\sin\theta_2\cos\theta_1\cos\theta_2 \\
& + 4\mathbf{X}^2c_a^2c_v^2x^2\cos\phi\sin\theta_1\sin\theta_2 \\
& + \mathbf{X}^2(c_v^2 + c_a^2)^2x^2(1 - \cos^2\theta_1\cos^2\theta_2 - \cos\phi\sin\theta_1\sin\theta_2\cos\theta_1\cos\theta_2) \\
& - 4\mathbf{P}^2c_a^2c_v^2(x^2 - 4)\cos\phi\sin\theta_1\sin\theta_2 \\
& + \mathbf{P}^2(c_v^2 + c_a^2)^2(x^2 - 4)(1 - \cos^2\theta_1\cos^2\theta_2 + \cos\phi\sin\theta_1\sin\theta_2\cos\theta_1\cos\theta_2)
\end{aligned}$$

## A.2 The special cases

In this appendix we list the triple differential cross section for pure Higgs spin and CP states. In addition we also give the differential cross sections, where some of the angular variables have been integrated over. F11, F12, F21, F22 refer to the different quadrants as defined in Chapter 4. The spin 0, CP even part only contains the pure SM contribution.

### Spin 0, CP even

$$\begin{aligned}
& \frac{d\sigma}{d\phi d\cos\theta_1 d\cos\theta_2} \sim + 16c_a^2c_v^2(2\cos\theta_1\cos\theta_2 + (x^2 - 2)\cos\phi\sin\theta_1\sin\theta_2) \\
& + (c_v^2 + c_a^2)^2\{4(1 + \cos^2\theta_1\cos^2\theta_2 + \cos^2\phi\sin^2\theta_1\sin^2\theta_2 \\
& + (x^2 - 2)\cos\phi\sin\theta_1\sin\theta_2\cos\theta_1\cos\theta_2) + x^2(x^2 - 4)\sin^2\theta_1\sin^2\theta_2\} \\
& \frac{d\sigma}{d\cos\theta_1 d\cos\theta_2} \sim + 32c_a^2c_v^2\cos\theta_1\cos\theta_2 \\
& + (c_v^2 + c_a^2)^2\{4(1 + \cos^2\theta_1\cos^2\theta_2) + (x^4 - 4x^2 + 2)\sin^2\theta_1\sin^2\theta_2\} \\
\text{F11} = \text{F22}: \frac{d\sigma}{d\phi} \sim & c_a^2c_v^2(8 + \pi^2(x^2 - 2)\cos\phi) \\
& + 4/9(c_v^2 + c_a^2)^2(x^4 - 4x^2 + 10 + (x^2 - 2)\cos\phi + 4\cos^2\phi) \\
\text{F12} = \text{F21}: \frac{d\sigma}{d\phi} \sim & - c_a^2c_v^2(8 - \pi^2(x^2 - 2)\cos\phi) \\
& + 4/9(c_v^2 + c_a^2)^2(x^4 - 4x^2 + 10 - (x^2 - 2)\cos\phi + 4\cos^2\phi)
\end{aligned}$$

### Spin 0, CP odd

$$\frac{d\sigma}{d\phi d \cos \theta_1 d \cos \theta_2} \sim + 8c_a^2 c_v^2 \cos \theta_1 \cos \theta_2 + (c_v^2 + c_a^2)^2 (1 + \cos^2 \theta_1 \cos^2 \theta_2 - \cos^2 \phi \sin^2 \theta_1 \sin^2 \theta_2)$$

$$\frac{d\sigma}{d \cos \theta_1 d \cos \theta_2} \sim + 16c_a^2 c_v^2 \cos \theta_1 \cos \theta_2 + (c_v^2 + c_a^2)^2 (1 + \cos^2 \theta_1) (1 + \cos^2 \theta_2)$$

$$F11 = F22: \frac{d\sigma}{d\phi} \sim c_a^2 c_v^2 + 1/9 (c_v^2 + c_a^2)^2 (5 - 2 \cos^2 \phi)$$

$$F12 = F21: \frac{d\sigma}{d\phi} \sim - c_a^2 c_v^2 + 1/9 (c_v^2 + c_a^2)^2 (5 - 2 \cos^2 \phi)$$

### Spin 1, CP even

$$\frac{d\sigma}{d\phi d \cos \theta_1 d \cos \theta_2} \sim + 4c_a^2 c_v^2 \cos \phi \sin \theta_1 \sin \theta_2 + (c_v^2 + c_a^2)^2 (1 - \cos^2 \theta_1 \cos^2 \theta_2 - \cos \phi \sin \theta_1 \sin \theta_2 \cos \theta_1 \cos \theta_2)$$

$$\frac{d\sigma}{d \cos \theta_1 d \cos \theta_2} \sim 1 - \cos^2 \theta_1 \cos^2 \theta_2$$

$$F11 = F22: \frac{d\sigma}{d\phi} \sim + c_a^2 c_v^2 \pi^2 \cos \phi + 1/9 (c_v^2 + c_a^2)^2 (32 - 4 \cos \phi)$$

$$F12 = F21: \frac{d\sigma}{d\phi} \sim + c_a^2 c_v^2 \pi^2 \cos \phi + 1/9 (c_v^2 + c_a^2)^2 (32 + 4 \cos \phi)$$

### Spin 1, CP odd

$$\frac{d\sigma}{d\phi d \cos \theta_1 d \cos \theta_2} \sim -4c_a^2 c_v^2 \cos \phi \sin \theta_1 \sin \theta_2 + (c_v^2 + c_a^2)^2 (1 - \cos^2 \theta_1 \cos^2 \theta_2 + \cos \phi \sin \theta_1 \sin \theta_2 \cos \theta_1 \cos \theta_2)$$

$$\frac{d\sigma}{d \cos \theta_1 d \cos \theta_2} \sim 1 - \cos^2 \theta_1 \cos^2 \theta_2$$

$$F11 = F22: \frac{d\sigma}{d\phi} \sim -c_a^2 c_v^2 \pi^2 \cos \phi + 1/9(c_v^2 + c_a^2)^2 (32 + 4 \cos \phi)$$

$$F12 = F21: \frac{d\sigma}{d\phi} \sim -c_a^2 c_v^2 \pi^2 \cos \phi + 1/9(c_v^2 + c_a^2)^2 (32 - 4 \cos \phi)$$

## References

- [1] Search for the Standard Model Higgs Boson at LEP, CERN-EP/2001-055 (2001).
- [2] For a short review of the Higgs search status at the LHC; F. Piccinini, contribution to ICHEP 2002, hep-ph/0209377 (2002).
- [3] D. Dominici, Riv. Nuovo Cim. **20**, 11 (1997).
- [4] B. Kastening and J. J. van der Bij Phys. Rev. **D60**: 095003 (1999).
- [5] A recent review; C. Quigg, Acta Phys. Polon. **B30**, 2145 (1999).
- [6] A. Abbasabadi and W. W. Repko, Nucl. Phys. **B292**, (1987) 461 and Phys. Rev. **D37**, (1988) 2668.
- [7] M. J. Duncan, Phys. Lett. **B179**, (1986) 393.
- [8] M. J. Duncan, G. L. Kane and W. W. Repko, Phys. Rev. Lett. **55**, (1985) 773 and Nucl. Phys. **B272**, (1986) 517.
- [9] J. R. Dell'Aquila and C. A. Nelson, Phys. Rev. **D33**, (1986) 80; C. A. Nelson, Phys. Rev. **D37**, (1988) 1220.
- [10] T. Matsuura and J. J. van der Bij, Z. Phys. **C51**, 259 (1991).
- [11] S. Y. Choi, D. J. Miller, M. M. Muhlleitner, P. M. Zerwas. CERN-TH/2002-231, DESY 02-150, PM/02-26. 2002
- [12] C. N. Yang Phys. Rev. **77**, 242 (1950).
- [13] H. L. Lai, J. Huston, S. Kuhlmann, F. Olness, J. Owens, D. Soper, W.K. Tung, H. Weerts. hep-ph/9606399. 1996
- [14] A. Djouadi, J. Kalinowski, M. Spira. DESY 87-079 or hep-ph/9704448. 1997
- [15] E. Richter-Was, D. Froidevaux, L. Poggiali. ATL-PHYS-98-131. 1998
- [16] Atlas Detector and Physics Performance. Technical Design Report. Volume 1. CERN 1999
- [17] Atlas Detector and Physics Performance. Technical Design Report. Volume 2. CERN 1999